JOURNAL OF GEOPHYSICAL RESEARCH, VOL. 102, NO. C7, PAGES 15,797–15,805, JULY 15, 1997

Spectral evolution of shoaling and breaking waves on a barred beach

Steve Elgar

Electrical Engineering and Computer Science, Washington State University, Pullman

R. T. Guza and B. Raubenheimer

Center for Coastal Studies, University of California, La Jolla

T. H. C. Herbers and Edith L. Gallagher

Department of Oceanography, Naval Postgraduate School, Monterey, California

Abstract. Field observations and numerical model predictions are used to investigate the effects of nonlinear interactions, reflection, and dissipation on the evolution of surface gravity waves propagating across a barred beach. Nonlinear interactions resulted in a doubling of the number of wave crests when moderately energetic (about 0.8-m significant wave height), narrowband swell propagated without breaking across an 80-m-wide, nearly flat (2-m depth) section of beach between a small offshore sand bar and a steep (slope = 0.1) beach face, where the waves finally broke. These nonlinear energy transfers are accurately predicted by a model based on the nondissipative, unidirectional (i.e., reflection is neglected) Boussinesq equations. For a lower-energy (wave height about 0.4 m) bimodal wave field, high-frequency seas dissipated in the surf zone, but lower-frequency swell partially reflected from the steep beach face, resulting in significant cross-shore modulation of swell energy. The combined effects of reflection from the beach face and dissipation across the sand bar and near the shoreline are described well by a bore propagation model based on the nondispersive nonlinear shallow water equations. Boussinesq model predictions on the flat section (where dissipation is weak) are improved by decomposing the wave field into seaward and shoreward propagating components. In more energetic (wave heights greater than 1 m) conditions, reflection is negligible, and the region of significant dissipation can extend well seaward of the sand bar. Differences between observed decreases in spectral levels and Boussinesq model predictions of nonlinear energy transfers are used to infer the spectrum of breaking wave induced dissipation between adjacent measurement locations. The inferred dissipation rates typically increase with increasing frequency and are comparable in magnitude to the nonlinear energy transfer rates.

Introduction

The evolution of surface gravity waves propagating across a natural, barred beach is examined by using existing models and new observations from a densely instrumented cross-shore transect. Shallow water waves evolve owing to shoaling (changes in group velocity $\mathrm{Cg}(f)$), nonlinear interactions, reflection from shore, and dissipation associated with wave breaking. On a beach with straight and parallel depth contours, waves refract to near-normal incidence in shallow water, and the cross-shore (x) evolution of the sea-surface elevation variance spectrum $E(f)$ can be expressed as

$$\frac{d(E(f)\mathrm{Cg}(f))}{dx} = N(f) + R(f) + D(f). \qquad (1)$$

Shoaling is incorporated in the left-hand side, nonlinear interactions ($N(f)$) primarily exchange energy between wave triads with frequencies $f = f_1, f_2$, and f_3, where $f_1 \pm f_2 \pm f_3 = 0$, reflection ($R(f)$) causes spatial modulations of $E(f)$ through phase coupling of incident and reflected waves, and dissipation ($D(f)$) removes energy from the wave field. Wind generation and bottom friction are considered negligible over the relatively short propagation distances (a few hundred meters) considered here. Many existing breaking wave transformation

Paper number 97JC01010.
0148-0227/97/97JC-01010$09.00

models use a bulk (frequency-integrated) version of the energy balance (1), neglect N and R, and use heuristic parameterizations for a bulk D [e.g., *Battjes and Janssen*, 1978; *Thornton and Guza*, 1983]. The consideration of energy spectra rather than bulk energy, and the incorporation of $N(f)$ (which requires higher-order statistics such as bispectra), $R(f)$ (which requires a complicated shoreline boundary condition [*Peregrine*, 1967]), and $D(f)$ (for which there is no accepted theory) complicates the model formulation.

Models based on the Boussinesq equations [*Peregrine*, 1967] predict accurately the relatively rapid nonlinear evolution observed in shallow water ($kh << 1$, where k is the wavenumber and h is the water depth) just seaward of the breaking region [*Freilich and Guza*, 1984; *Elgar et al.*, 1990; and many others]. In these previous studies the beaches were monotonically and moderately sloping, and significant nonlinear evolution of unbroken waves was restricted to a narrow region limited by increasing depth offshore and wave breaking onshore. Stronger nonlinear evolution prior to breaking was sometimes observed in the present study because nonbreaking waves propagated over a wide (80 m), shallow (2 m deep), flat section of beach between an offshore sand bar and the steep beach face. For cases of narrowband swell there were twice as many distinct wave crests near the beach face as in deeper water. Although the theory is well established [*Mei and Ünlüata*, 1972], detailed field measurements of this nonlinear phenomenon have not been reported. In the present study, strong nonlinear evolution of nonbreaking swell observed on a natural beach is shown to be described well by the Boussinesq equations.

Although the shoreline reflection of infragravity frequency (approximately $0.001 < f < 0.05$ Hz) waves is significant [*Suhayda*, 1974; *Huntley et al.*, 1981; *Guza et al.*, 1984; and others], reflection of swell from natural beaches is often considered negligible. However, the steep foreshore of the beach studied here partially reflected low energy swell. Nonlinear interactions between incident and reflected components are far from resonance, and thus do not contribute to $N(f)$. However, the interference of incident and reflected waves causes partial standing wave patterns with observed swell wave heights modulated by as much as a factor of 2. Here, colocated velocity and pressure measurements are used to separate the observed wave field into incident and reflected components. In a low-energy, bimodal wave field the combined effects of reflection of swell from the beach face and dissipation of higher-frequency sea across the sand bar and flat section are described well by a bore propagation model [*Kobayashi et al.*, 1989; *Kobayashi and Wurjanto*, 1992] based on the nondispersive nonlinear shallow water equations.

Breaking-induced dissipation and nonlinear interactions dominate the spectral evolution of energetic wave fields. Guided by laboratory observations and Boussinesq model predictions, *Mase and Kirby* [1992] and *Kaihatu and Kirby* [1995] suggested that the normalized dissipation rate $D(f)/E(f)$ increases with frequency, whereas on the basis of different laboratory observations, *Beji and Battjes* [1993] and *Eldeberky and Battjes* [1996] conclude that the relative dissipation rate is frequency independent. In the present study, energy-conserving Boussinesq equations are used to predict spectral changes (between closely spaced pairs of wave gages) resulting from nonlinear energy transfers. Discrepancies between observed and predicted spectral changes are attributed to breaking-induced dissipation [*Ferriole*, 1991]. The inferred dissipation rates in the surf zone are shown to increase with increasing frequency, in qualitative agreement with *Mase and Kirby* [1992] and *Kaihatu and Kirby* [1995].

The field experiment is described next, followed by discussion of selected case studies illustrating the effects of nonlinear interactions, reflection, and dissipation on shoaling and breaking waves.

Field Experiment and Data Reduction

The data were obtained during the Duck94 nearshore field experiment conducted near Duck, North Carolina, on a barrier island exposed to the Atlantic ocean. Colocated sonar altimeters (to determine the location of the seafloor [*Gallagher et al.*, 1996]), pressure sensors, and bidirectional electromagnetic current meters were deployed on a 750-m-long cross-shore transect extending from the shoreline to 8-m water depth (Figure 1a) and were sampled at 2 Hz. For each 3-hour-long case study, sea-surface elevation spectra with 120 degrees of freedom were estimated from overlapped (75%), detrended, Hanning windowed, 512-s-long pressure records using a linear theory depth correction. The directional spectrum of swell and sea was estimated with data from a two-dimensional array of 15 bottom pressure sensors located in 8-m water depth (not shown) [*Long*, 1996].

Changes in the beach profile were small during the 2 weeks in September when the observations discussed here were obtained (Figure 1a). The depth decreased gradually (slope of ≈ 0.01) from 8 m to a small sand bar in about 2-m depth ($x \approx 240$ m, Figure 1a). The bottom was nearly horizontal (less than 30-cm depth variation) between the sand bar and a steep (slope of ≈ 0.1) beach face ($135 < x < 160$ m, Figure 1a). Mean water depths over the flat section ranged between about 170 and 250 cm, depending on tidal stage. Longshore depth variations are neglected here.

Observations

Four data runs representative of the wide range of observed wave evolution are discussed here. In 8-m depth the significant wave heights (H_s) ranged from 0.4 to 2.7 m (Figure 1b), and the peak frequencies ranged from 0.06 to 0.12 Hz (Figure 2). The spectrum in 8-m depth for the smallest waves ($H_s = 0.4$ m, run 09141900) is bimodal with roughly equal energy in two narrow peaks at 0.06 and 0.11 Hz. Two cases with moderately energetic swell ($H_s = 0.8$ m, 09061600, and $H_s = 1.3$

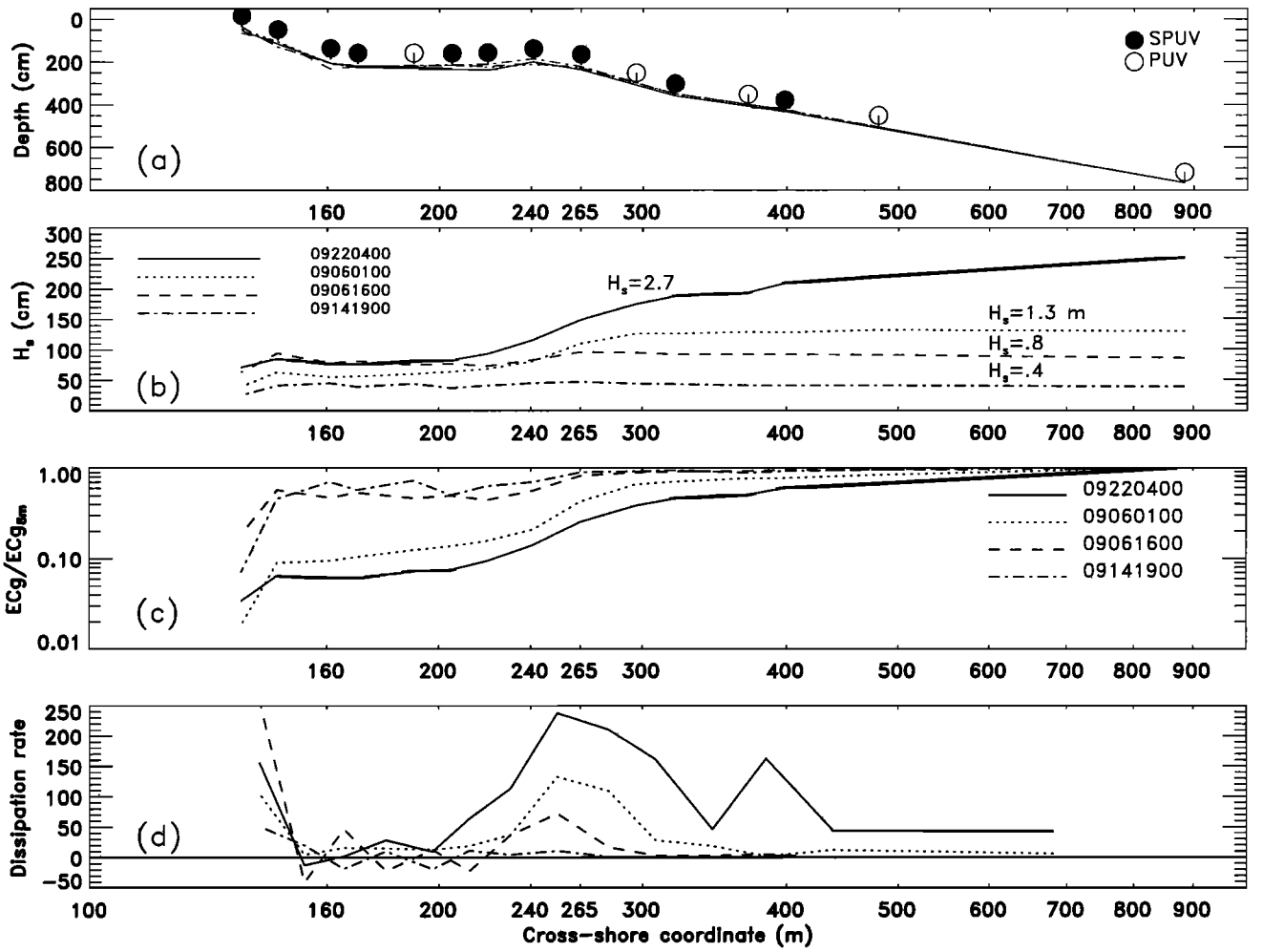

Figure 1. (a) Cross-shore beach profiles (depth below mean sea level) for each case study and locations of instruments. Solid circles indicate a colocated sonar altimeter (S), pressure gage (P), and electromagnetic current meter (UV). Open circles indicate a colocated pressure gage and electromagnetic current meter. (b) Significant wave height. (c) Ratio of the total energy flux ECg (2) to the total offshore energy flux (observed in 8-m water depth) $E\mathrm{Cg}_{8\mathrm{m}}$. (d) Bulk dissipation rate $(E\mathrm{Cg}(x+\Delta x)-E\mathrm{Cg}(x)/\Delta x$ (arbitrary units), where x and $x+\Delta x$ are the cross-shore coordinates of adjacent instruments) versus the logarithm of the cross-shore coordinate. The data run name (indicated in the legend) format is mmddhhhh, where mm is month, dd is day, and hhhh is hour (EST) of the beginning of the 3-hour record.

m, 09060100) have unimodal spectra with a peak frequency of 0.085 Hz. The spectrum of the most energetic wave field ($H_s = 2.7$ m, 09220400), observed during a nor'easter, is broader with a maximum at higher frequency ($f \approx 0.12$ Hz). In all four cases, waves in 8-m depth with frequencies near the spectral peak approached the beach within about 20° of normal incidence, and oblique propagation effects are neglected.

There was little dissipation between 8-m depth and the seaward edge of the sand bar ($x = 265$ m, Figure 1a) for the two cases with the least energetic waves (09141900 and 09061600), resulting in nearly constant H_s (Figure 1b) and only a small decrease in the total energy flux ECg in relation to the flux $E\mathrm{Cg}_{8\mathrm{m}}$ in 8-m depth (Figure 1c). The total flux was calculated from the observations (assuming shoreward progressive waves) by integrating the energy flux over the swell-sea frequency band (nominally $0.05 \le f \le 0.24$ Hz),

$$E\mathrm{Cg} = \int_{0.05\mathrm{Hz}}^{0.24\mathrm{Hz}} E(f)\mathrm{Cg}(f)df \qquad (2)$$

The bulk dissipation rate $((E\mathrm{Cg}(x+\Delta x)-E\mathrm{Cg}(x))/\Delta x$ estimated from observations at adjacent instrument pairs Δx apart) in these two low-energy cases is close to 0 seaward of the sand bar, increases over the bar where 20-40% of the incident energy flux is dissipated, and then oscillates slightly about zero (possibly owing to reflection) before the waves break on the beach face (Figure 1d). In more energetic conditions ($H_s = 1.3$ m, 09060100), intense wave breaking occurs near the bar crest, and ECg is reduced by about an order of mag-

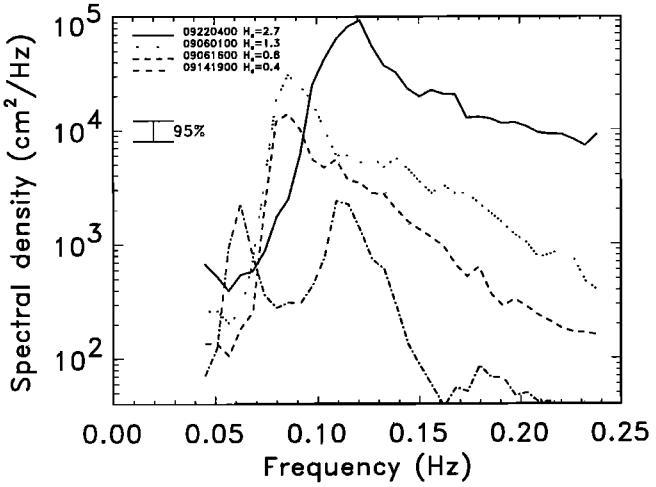

Figure 2. Sea-surface elevation spectral density in 8-m depth versus frequency for the four case studies. The bars are 95% confidence levels (120 degrees of freedom).

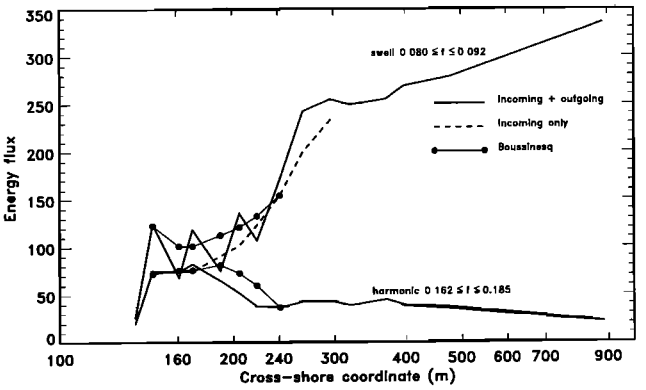

Figure 4. Energy flux ECg (2) (arbitrary units) integrated over the swell ($0.080 \leq f \leq 0.092$ Hz, upper curves) and harmonic ($0.162 \leq f \leq 0.185$ Hz, lower curves) frequency bands versus cross-shore coordinate for run 09061600: observed incoming plus outgoing waves (solid curves), observed incoming-only waves (dashed curves), and Boussinesq model predictions initialized at $x = 240$ m with incoming-only waves (solid circles). Reflection at harmonic frequencies is weak, so the dashed and solid curves are indistinguishable for the harmonic frequency band.

nitude. Significant breaking-induced dissipation of the most energetic waves ($H_s = 2.7$ m, 09220400) extends well seaward of the bar.

Nonlinear Interactions

Nonlinear transfers of energy to higher frequencies can affect dramatically both the spectrum and the shapes of the waves, as illustrated by the evolution of narrowband swell ($H_s = 0.8$ m, run 09061600). Significant nonlinear transfer of energy from the incident swell ($f = 0.085$ Hz) to its harmonic ($f = 0.170$ Hz) occurred between 8-m depth and the sand bar, and in particular across the flat section, resulting in comparable energy in the swell and harmonic frequency bands at the beach face toe ($x = 160$ m in Figures 3 and 4). There were about twice as many distinct wave crests at the toe as near the bar crest (Figure 5), similar to previous visual and video observations of narrowband swell shoaling over a barred beach [*Byrne*, 1969]. These cumulatively large energy transfers to harmonic frequencies are usually not observed on monotonically sloping sandy beaches, where the nonlinear evolution to breaking occurs over a much shorter distance. The shapes of the waves, quantified statistically by the skewness (crest-trough asymmetry, for example, sharp peaks and

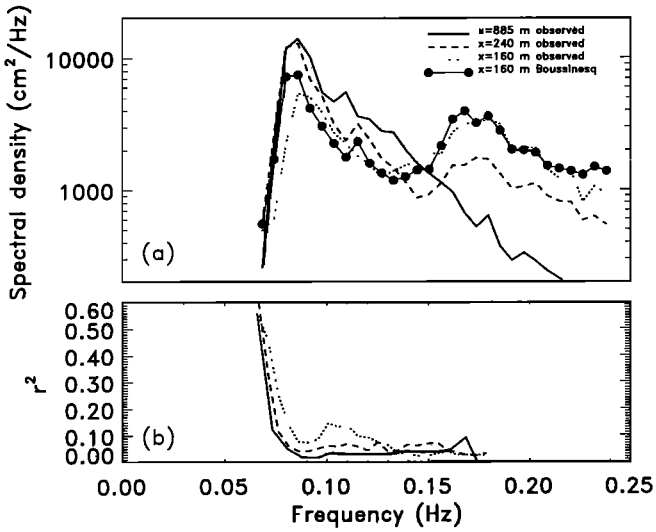

Figure 3. (a) Sea-surface elevation spectral density versus frequency for the 09061600 run observed at $x = 885$ (solid curve), $x = 240$ (dashed curve), and $x = 160$ m (dotted curve), and predicted by the Boussinesq model (initialized with observations at $x = 240$ m) at $x = 160$ m (thin solid curve with solid circles). (b) Corresponding squared reflection coefficient (ratio of seaward to shoreward propagating wave energy) observed at $x = 885$, 240, and 160 m.

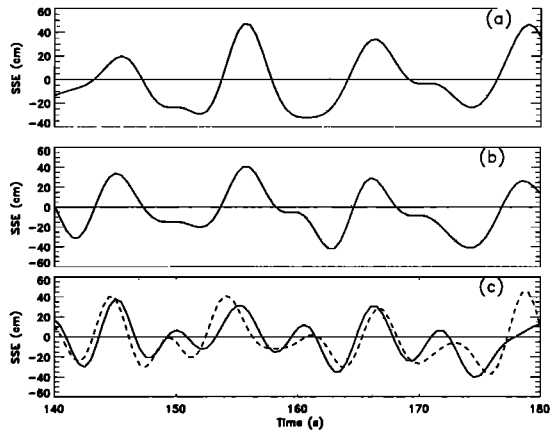

Figure 5. Sea-surface elevation (incoming-only waves) for run 09061600 versus time, observed at (a) $x = 885$, (b) $x = 240$, and (c) $x = 160$ (solid curves) and predicted at $x = 160$ m by the Boussinesq model (dashed curve in Figure 5c) initialized with incoming-only waves observed at $x = 240$ m.

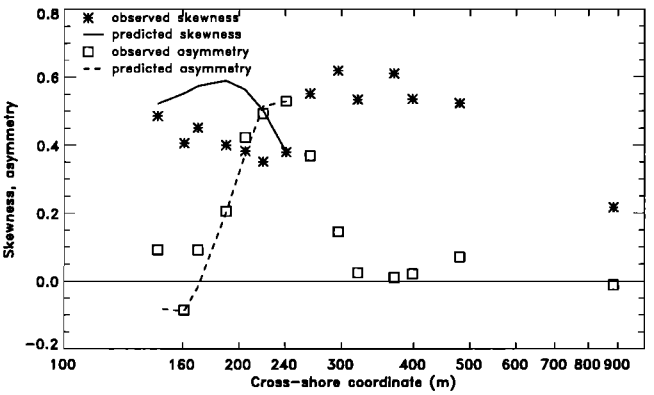

Figure 6. Sea-surface elevation skewness and asymmetry versus cross-shore coordinate for run 09061600: observed skewness (asterisks) and asymmetry (squares) and Boussinesq model predictions (initialized at x = 240 m) of the skewness (solid curve) and asymmetry (dashed curve).

flat troughs) and asymmetry (fore-aft asymmetry, for example, steep front faces and gently sloping rear faces) also evolved significantly. The skewness and asymmetry increased from near zero in 8-m water depth (where the waves were nearly symmetric) to about 0.5 at the crest of the sand bar (Figure 6). Across the flat section the skewness remained nearly constant, but the asymmetry decreased to approximately zero. Similar cross-shore evolution of wave spectra and shapes has been observed in laboratory experiments [*Elgar et al.*, 1992; *Ohyama and Nadaoka*, 1994; *Ohyama et al.*, 1994].

The observed nonlinear changes in the spectrum and wave shapes are predicted qualitatively well by a model [*Freilich and Guza*, 1984] based on the Boussinesq equations [*Peregrine*, 1967]. Visual observations indicated spilling of some wave crests over the sand bar ($240 < x < 265$ m), but less breaking over the shallow flat seafloor between the bar crest and the toe of the steep beach face (x = 160 m). Therefore the model, which does not include dissipation, was initialized with time series of sea-surface elevation observed just shoreward (x = 240 m) of the bar crest (Figures 3, 4, and 6). The Boussinesq model assumes slowly varying depth and unidirectional normally incident waves, and thus does not account for partial reflection of swell from the steep beach face ($r^2 \approx 0.1$ at the swell peak in Figure 3b, where the squared reflection coefficient r^2 is the ratio of seaward to shoreward propagating energy) apparent in cross-shore standing wave patterns of nodes and antinodes (Figure 4). If reflection is not accounted for, model predictions are sensitive to the location (in relation to nodes and antinodes) of the model initial conditions. Time series of incident and reflected waves were therefore estimated from each pressure-current meter pair using linear longwave theory [*Nagata*, 1964; *Guza et al.*, 1984]. The Boussinesq model was initialized with progressive shoreward propagating wave components and compared with observed shoreward propagating waves. The reflected waves have relatively small amplitudes, and triad interactions involving directionally opposing wave components are far from resonance. Thus, nonlinear interactions between outgoing or between incoming and outgoing waves are expected to be negligible. The predicted decrease in shoreward propagating swell energy owing to nonlinear interactions is somewhat less than the observed decrease (Figure 4), possibly because dissipation is neglected. Nevertheless, the observed decrease in swell energy and increase in harmonic energy at shoreward locations that results in twice as many waves at the toe of the beach face is predicted by the Boussinesq model (Figures 3, 4, and 5c).

Reflection

Reflection of a small fraction of the incident wave energy flux produces significant cross-shore variations in energy levels. For example, the weak reflection observed for the 09061600 case (Figure 3b) resulted in swell energy fluctuations of almost a factor of 2 across the flat section of beach (Figure 4).

Cross-shore energy fluctuations are even more pronounced for the lower-energy (H_s = 0.4 m) mixed swell and sea case (09141900) (Figures 7 and 8), where the reflection coefficient of swell was close to 1 near the beach face. The reflection causes partial standing wave patterns with nearly a factor of 4 fluctuation in swell variance across the flat section of beach (Figure 8a). In 2-m water depth the wavelength of 0.06 Hz swell is about 74 m, so the expected separation of nodes and antinodes is about 74/4=18 m. The 10- to 20-m separation between sensors on the flat section (Figure 1a) is thus too large to resolve the swell energy modulation. Smaller reflection coefficients observed offshore of the sand bar (Figure 7b) are consistent with partial dissipation of incident swell on the bar [*Raubenheimer and Guza*, 1996]. Reflection coefficients were small at frequencies greater than 0.1 Hz.

The observed reflection of swell and dissipation of sea is predicted qualitatively by the model Rbreak [*Kobayashi et al.*, 1989; *Kobayashi and Wurjanto* 1992] based on the nonlinear shallow water equations (Figures 7 and 8). As implemented here [*Raubenheimer and Guza*, 1996], the model is initialized with observations of sea-surface elevation and cross-shore current fluctuations (i.e., predicted and observed reflection are equal at the seaward boundary), and thus is insensitive to the proximity of the initial conditions to nodes or antinodes. Large discrepancies between predicted and observed spectral levels for frequencies above about 0.12 Hz (Figure 7) suggest that dispersion effects neglected in Rbreak are important to spectral evolution at higher frequencies.

The transfer of energy from incident swell and sea to higher frequencies (where reflection is weak) is predicted accurately by the Boussinesq model, which does not account for reflection or dissipation, but includes weak dispersion (Figure 8c). The model was initialized with the shoreward propagating wave field at x = 240 m, shoreward of the region of greatest dissipation (over the crest of the sand bar, $240 < x < 265$ m, especially for sea frequencies, Figure 8b). Although the Boussinesq model does not predict the observed cross-shore energy

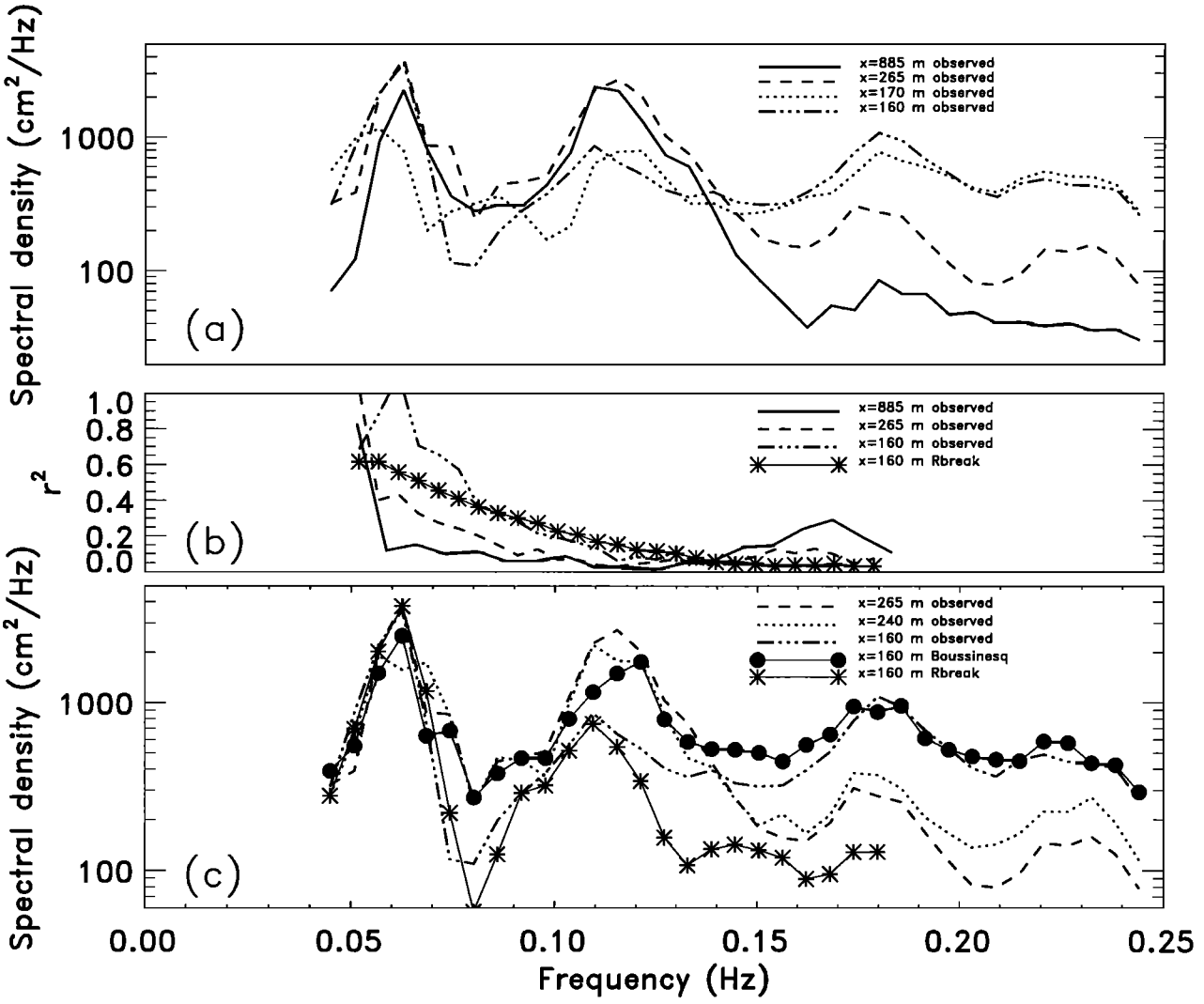

Figure 7. (a) Sea-surface elevation spectral density versus frequency observed for run 09141900 at $x = 885, 265, 170$, and 160 m. (b) Corresponding squared reflection coefficient (ratio of seaward to shoreward propagating energy) observed at $x = 885, 265$, and 160 m and predicted by Rbreak at $x = 160$ m. (c) Sea-surface elevation spectral density observed at $x = 265, 240$, and 160 m and predicted at $x = 160$ m using Boussinesq (initialized at $x = 240$ m with incoming-only waves) and Rbreak (initialized at $x = 265$ m with the total sea-surface elevation (incoming and reflected waves)) models.

modulations owing to partial standing waves, the predicted decrease in shoreward energy flux at swell and sea frequencies (Figures 8a and 8b, respectively) and the increase in energy at their sum frequency (Figure 8c) are in reasonable agreement with the observations.

Dissipation

For more energetic swell ($H_s \geq 1$ m) the observed reflection is typically negligible, and wave evolution is dominated by dissipation and nonlinear interactions. In run 09060100 the significant wave height decreased from 1.3 m in 8-m depth to 0.5 m just shoreward of the sand bar ($x = 240$ m, Figure 1), corresponding to a factor of 5 reduction in energy flux. Spectral levels decreased monotonically at most frequencies as the waves propagated from $x = 296$ m across the sand bar to the beach face (Figure 9a).

The dissipation rate $D(f)$ was calculated from (1) by neglecting reflection, estimating nonlinear energy transfers $N(f)$ with the (nondissipative) Boussinesq model, and attributing to dissipation the residual changes in the observed energy flux,

$$D(f) \approx \frac{\Delta(E_{\mathrm{obs}}(f)\mathrm{Cg}(f))}{\Delta x} - N(f) \qquad (3)$$

where $\Delta(E_{\mathrm{obs}}(f)\mathrm{Cg}(f))$ is the difference between energy fluxes observed at adjacent instrument locations x and $x + \Delta x$. For small Δx the nonlinear transfer between the two measurement locations predicted by the Boussinesq equations is

$$N(f)\Delta x \approx E_{\mathrm{obs},x}(f)\mathrm{Cg}(f) - E_{\mathrm{Bous},x+\Delta x}(f)\mathrm{Cg}(f) \quad (4)$$

where $E_{\mathrm{Bous},x+\Delta x}(f)$ is the spectrum at $x + \Delta x$ pre-

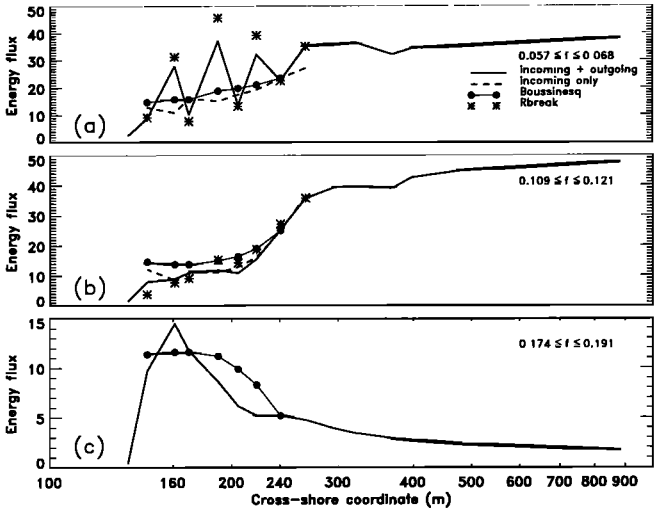

Figure 8. Band-integrated energy flux (2) (arbitrary units) versus cross-shore coordinate for run 09141900. Integration limits are (a) $0.057 \leq f \leq 0.068$, (b) $0.109 \leq f \leq 0.121$, and (c) $0.174 \leq f \leq 0.191$ Hz. Solid curves are observed total (incoming plus outgoing) waves, and dashed curves (Figures 8a and 8b) are observed incoming-only waves. Solid circles are Boussinesq model predictions initialized at $x = 240$ m with incoming-only waves, and asterisks in Figures 8a and 8b are Rbreak model predictions initialized at $x = 265$ m.

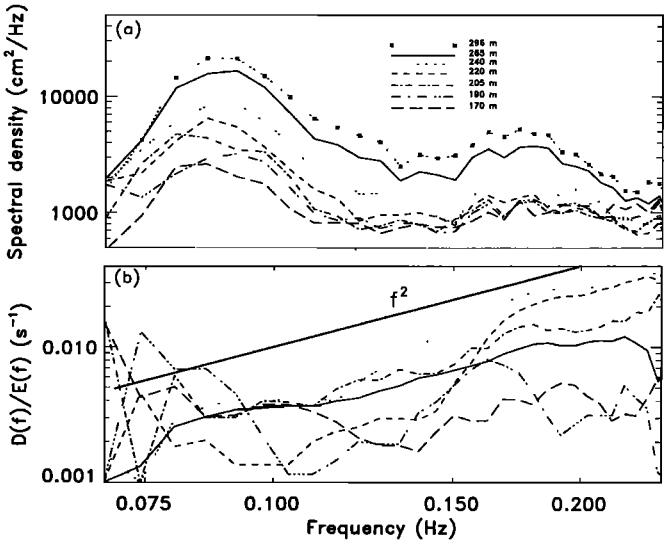

Figure 9. (a) Observed sea-surface elevation spectral density versus frequency for run 09060100 (see legend for observation locations). (b) Normalized energy dissipation rate versus frequency. The thick, smooth solid line is proportional to f^2. The dissipation rate between two sensors is plotted with a line type in Figure 9b corresponding to the line type of the shallower sensor of the pair in Figure 9a.

dicted by the Boussinesq model initialized with observations at x. Thus,

$$D(f)\Delta x \approx E_{\mathrm{Bous},x+\Delta x}(f)\mathrm{Cg}(f) - E_{\mathrm{obs},x+\Delta x}(f)\mathrm{Cg}(f) \quad (5)$$

Similar to the laboratory results of *Mase and Kirby* [1992] and *Kaihatu and Kirby* [1995], the inferred normalized dissipation rate $D(f)/E(f)$ increases with frequency (roughly proportional to f^2) except near the most shoreward locations, where dissipation is small (Figure 9b). Errors in the estimates of $D(f)$ are introduced if Δx is large because the Boussinesq model does not account for the dissipation between adjacent measurement locations or the associated reduction in nonlinear energy transfers, resulting in artificially high inferred dissipation rates at high frequencies. Analysis of the same data with a Boussinesq model that explicitly includes dissipation [Chen et al., Modeling breaking surface waves in shallow water, submitted to *Journal of Geophysical Research*, 1997] (the model is similar to that of *Mase and Kirby* [1992]) suggests that the sensor spacing is not so large as to affect significantly the inferred dissipation rates at high frequencies.

For $265 < x < 296$ m there is little nonlinear evolution of the spectrum near the swell peak ($f = 0.085$ Hz), but there is significant inferred dissipation (Figure 10a). At shoreward locations, nonlinear interactions transfer energy from the spectral peak to higher frequencies, as indicated by the change in sign of $N(f)$ between the spectral peak and its harmonic in Figure 10. At frequencies near the harmonic ($f = 0.170$ Hz) significant energy gain from nonlinear transfers nearly balances losses from dissipation, resulting in only a slight net energy decrease. The inferred frequency-dependent dissipation rate $D(f)$ is typically within a factor of 3 of the nonlinear energy transfer $N(f)$ (Figure 10). Although

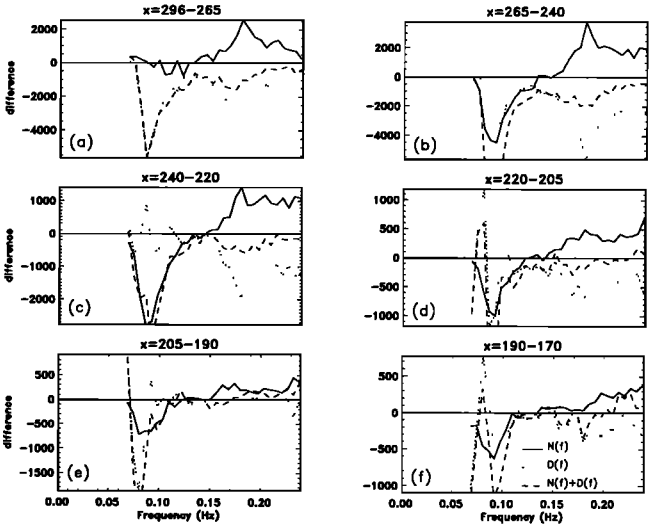

Figure 10. Theoretical nonlinear energy transfers $N(f)$ (solid curves, (4)) and estimated dissipation $D(f)$ (dotted curves, (5)) between pairs of sensors versus frequency for run 09060100. Dashed curves indicate the measured net change $N(f) + D(f)$. The cross-shore locations of the two sensors are (a) $x = 296$ and $x = 265$, (b) 265 and 240, (c) 240 and 220, (d) 220 and 205, (e) 205 and 190, and (f) 190 and 170 m. Inferred "negative" dissipation (i.e., $D(f) > 0$, e.g., $0.07 \leq f \leq 0.09$ Hz in Figures 10c-10f) may be the result of neglected reflected waves.

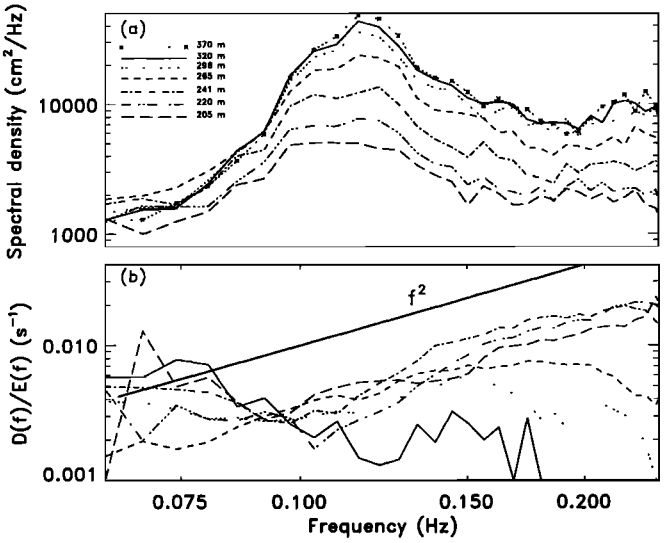

Figure 11. (a) Observed sea-surface elevation spectral density versus frequency for run 09220400 (see legend for observation locations). (b) Normalized energy dissipation rate versus frequency. The thick, smooth solid line is proportional to f^2. The dissipation rate between two sensors is plotted with a line type in Figure 11b corresponding to the line type of the shallower sensor of the pair in Figure 11a.

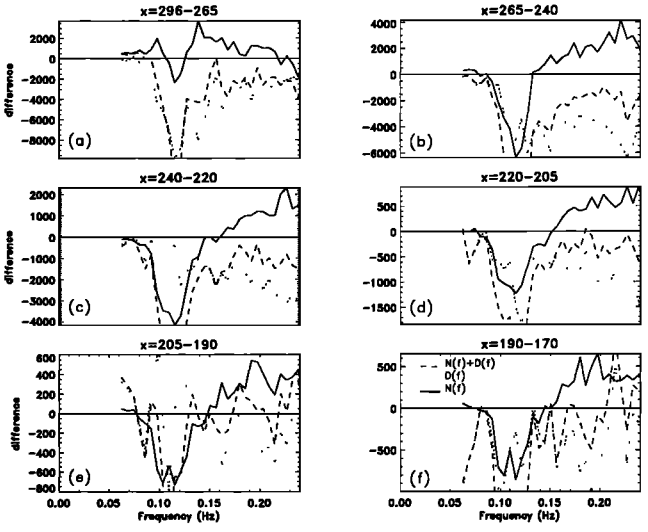

Figure 12. Theoretical nonlinear energy transfers $N(f)$ (solid curves, (4)) and estimated dissipation $D(f)$ (dotted curves, (5)) between pairs of sensors versus frequency for run 09220400. Dashed curves indicate the measured net change $N(f) + D(f)$. The cross-shore locations of the two sensors are (a) $x = 296$ and $x = 265$, (b) 265 and 240, (c) 240 and 220, (d) 220 and 205, (e) 205 and 190, and (f) 190 and 170 m.

dissipation is cumulatively the dominant term, nonlinearity can locally be nearly as large as dissipation.

The spatial evolution of spectra of the most energetic waves ($H_s = 2.7$, run 09220400) is shown in Figures 11 and 12. Dissipation rates were greater than those for the data sets discussed above (Figure 1), particularly over the sand bar ($240 < x < 265$ m, Figure 1d). Only about 10% of the incident energy flux reached $x = 240$ m (Figure 1c). In the outer surf zone (between $x = 370$ and $x = 265$ m) the inferred dissipation rates are only weakly frequency dependent, but closer to shore $D(f)/E(f)$ increases with frequency (roughly as f^2, Figure 11b). Local changes in spectral levels resulting from nonlinear interactions are of the same order as those caused by dissipation (Figure 12).

Conclusions

Shoaling surface waves in the swell-sea frequency band (0.05 to 0.24 Hz) evolve owing to variable depth, nonlinear interactions, reflection from the beach face, and dissipation. Nonlinear interactions result in cross-spectral energy transfers and evolving wave shapes. Large nonlinear energy transfers produced twice as many wave crests near the beach face as offshore when moderately energetic, nearly breaking swell propagated over a shallow (2-m depth), flat section of the beach. The highly asymmetric (pitched forward) and skewed (sharp peaks) wave shapes near the seaward edge of the flat section became nearly symmetrical (although still skewed) at the shoreward edge. A Boussinesq model predicts this observed evolution.

Low-frequency, lower-energy swell partially reflected from the beach face, causing partial standing waves and cross-shore variations in swell energy. A model based on the nondispersive, nonlinear shallow water equations predicts accurately the observed partial reflection of swell, and the stronger dissipation of sea, although the depth and frequency ranges for which this model is valid are limited by dispersion. The agreement between these observations and Boussinesq model predictions (based on the assumption of no reflection) is improved by separating the observed wave field into incident and reflected components.

The evolution of more energetic wave fields was influenced strongly by breaking-induced dissipation. The underlying dynamics are not yet well understood, but a dissipation rate as a function of frequency was estimated by attributing to dissipation the difference between the observed decrease in energy flux and nonlinear energy transfers predicted by the (nondissipative) Boussinesq model. Although they are only a crude approximation, limited by finite sensor spacing and modeling assumptions not necessarily met by the observations, the inferred dissipation rates for these data sets are comparable in magnitude to the nonlinear energy transfer and are qualitatively consistent with a previously suggested increase of normalized dissipation rates with increasing frequency.

Acknowledgments. This research was supported by the Office of Naval Research (Coastal Dynamics, Nonlinear Ocean Waves ARI, and AASERT graduate student support) and the National Science Foundation (CoOP program). The extensive cross-shore transect of sensors was designed, con-

structed, deployed, and then recovered, repaired, and redeployed (after being damaged by lightning) by staff from the Center for Coastal Studies. Their tenacity and significant contribution to the Duck94 field experiment is greatly appreciated. The Field Research Facility, Coastal Engineering Research Center, Duck, North Carolina, provided excellent logistical support. M. H. Freilich made many valuable comments.

References

Battjes, J., and J. Janssen, Energy loss and set-up due to breaking of random waves, *Proc. Int. Coastal Eng. Conf. 16th*, 569–587, 1978.

Beji, S., and J. Battjes, Experimental investigation of wave propagation over a bar, *Coastal Eng., 19*, 151–162, 1993.

Byrne, R., Field occurrences of induced multiple gravity waves, *J. Geophys. Res., 74*, 2590–2596, 1969.

Eldeberky, Y., and J. A. Battjes, Spectral modeling of wave breaking: Application to Boussinesq equations, *J. Geophys. Res., 101*, 1253-1264, 1996.

Elgar, S., M.H. Freilich, and R.T. Guza, Model-data comparisons of moments of nonbreaking shoaling surface gravity waves, *J. Geophys. Res., 95*, 16,055–16,063, 1990.

Elgar, S., R.T. Guza, and M.H. Freilich, Dispersion, nonlinearity, and viscosity in shallow-water waves: Model results and laboratory comparisons, *J. Waterw. Port Coastal Ocean Eng., 119*, 351–366, 1992.

Ferriole, M., Laboratory observations of the evolution of surface gravity waves through the shoaling and breaking regions and the surf zone, M.S. thesis, Wash. State Univ. Pullman, 1991.

Freilich, M.H., and R.T. Guza, Nonlinear effects on shoaling surface gravity waves, *Philos. Trans. R. Soc. London Ser. A, 311*, 1–41, 1984.

Gallagher, E., B. Boyd, S. Elgar, R.T. Guza, and B.T. Woodward, Performance of a sonar altimeter in the nearshore, *Mar. Geol. 133*, 241–248, 1996.

Guza, R.T., E.B. Thornton, and R.A. Holman, Swash on steep and shallow beaches, *Proc. Int. Coastal Eng. Conf. 19th*, 708–723, 1984.

Huntley, D., R.T. Guza, and E. Thornton, Field observations of surf beat, 1, Progressive edge waves, *J. Geophys. Res., 89*, 1913-1920, 1981.

Kaihatu, J., and J. Kirby, Nonlinear transformation of waves in finite water depth, *Phys. Fluids, 7*, 1903–1914, 1995.

Kobayashi, N., and A. Wurjanto, Irregular wave setup and run-up on beaches, *J. Waterw. Port Coastal Ocean Eng., 118*, 368-386, 1992.

Kobayashi, N., G. S. DeSilva, and K. D. Watson, Wave transformation and swash oscillation on gentle and steep slopes, *J. Geophys. Res., 94*, 951-966, 1989.

Long, C., Index and bulk parameters for frequency-direction spectra measured at CERC Field Research Facility, June 1994 to August 1995, Misc. Pap. CERC-96-6, U.S. Army Eng. Waterw. Exp. Stn., Vicksburg, Miss., 1996.

Mase, H., and J. Kirby, Hybrid frequency-domain KdV equation for random wave transformation, *Proc. Int. Coastal Eng. Conf. 23rd*, 474–487, 1992.

Mei, C.C., and U. Ünlüata, Harmonic generation in shallow water waves, in *Waves on Beaches*, edited by R. E. Meyer, pp. 181-202, Academic, San Diego, Calif., 1972.

Nagata, Y., The statistical properties of orbital wave motions and their application for the measurement of directional wave spectra, *J. Oceanogr. Soc. Jpn., 19*, 169–181, 1964.

Ohyama, T., and K. Nadaoka, Transformation of a nonlinear wave train passing over a submerged shelf without breaking, *Coastal Eng., 24*, 1–22, 1994.

Ohyama, T., S. Beji, K. Nadaoka, and J. Battjes, Experimental verification of numerical model for nonlinear wave evolution, *J. Waterw. Port Coastal Ocean Eng., 120*, 637–644, 1994.

Peregrine, D.H., Long waves on a beach, *J. Fluid Mech., 27*, 815–827, 1967.

Raubenheimer, B., and R.T. Guza, Observations and predictions of runup, *J. Geophys. Res., 101*, 25,575–25,587, 1996.

Suhayda, J.N., Standing waves on beaches, *J. Geophys. Res., 72*, 3065–3071, 1974.

Smith, J., and C. Vincent, Shoaling and decay of two wave trains on a beach, *J. Waterw. Port Coastal Ocean Eng., 118*, 517–533, 1991.

Thornton, E., and R.T. Guza, Transformation of wave height distribution, *J. Geophys. Res., 88*, 5925-5938, 1983.

S. Elgar, Electrical Engineering and Computer Science, Washington State University, Pullman, WA 99164-2752. (e-mail: elgar@eecs.wsu.edu)

E. L. Gallagher and T. H. C. Herbers, Department of Oceanography, Naval Postgraduate School, Monterey, CA 93943.

R. T. Guza and B. Raubenheimer, Center for Coastal Studies 0209, University of California, La Jolla, CA 92093.

(Received May 31, 1996; revised December 6, 1996; accepted February 27, 1997.)